NASA
Technical
Paper
2413
C.2
April 1985

Semianalytic Modeling of Aerodynamic Shapes

Raymond L. Barger
and Mary S. Adams

NASA

NASA Technical Paper 2413

1985

Semianalytic Modeling of Aerodynamic Shapes

Raymond L. Barger
and Mary S. Adams

Langley Research Center
Hampton, Virginia

National Aeronautics
and Space Administration

Scientific and Technical Information Branch

Summary

Equations for the semianalytic representation of a class of surfaces that vary smoothly in cross-sectional shape are presented. Some methods for fitting together and superimposing such surfaces are described. A brief discussion is also included of the application of the theory in various contexts such as computerized lofting of aerodynamic surfaces and grid generation.

Introduction

A very general class of surfaces can be approximated for computational purposes by a set of flat panels or of curved patches (ref. 1). Aside from the storage and accounting problems of defining and retaining the information for each panel, such representations present difficulties for applications that require continuity of derivatives at the panel edges. The more stringent the smoothness requirement at the edge, the higher the order of the polynomial that is required for the modeling. This type of polynomial modeling leads to a surface "waviness" that may be difficult to detect visually but manifests itself in an oscillation of the derivatives.

This problem does not exist for simple configurations that can be synthesized from basic geometric shapes for which exact analytic descriptions are known. However, for aerodynamic configurations, this limitation to basic shapes is too restrictive for meaningful design. The present paper explores a somewhat different approach—one that retains many of the advantages of fully analytic representation while enlarging the class of shapes representable beyond simple geometric objects to include aerodynamic-type surfaces. A brief description is included of some advantages of the method relative to several problems: computerized lofting of aerodynamic shapes (both external and internal) and gridding for flow-field calculations. The procedure is a generalized version of a method described in reference 2.

Symbols

A	surface area
c	shape transition function
E, F, G	metric coefficients
$\hat{i}, \hat{j}, \hat{k}$	orthonormal base vectors
m	exponent parameter (eq. (5))
$\hat{N}$	unit surface normal vector
$\mathbf{r}$	surface vector
R, θ	polar coordinates
t	independent variable used to define surface cross-sectional shape
t_ℓ	parameter defined by equation (29)
x, y, z	Cartesian coordinates
x_m	$= 1 - x_3$
η	independent variable used for two-dimensional grid generation
λ	size transition function
μ	homotopy function of ξ
ξ	independent variable used for three-dimensional grid generation

Subscripts:

1,2,3	various cross-sectional shapes used in defining transition surface
a, b, c	quantities associated with different surfaces
f	fuselage surface
i	inner boundary
l	limiting
n	normalized
o	outer boundary
s	canopy surface
t, x	derivative with respect to t or x, respectively

An asterisk (*) with a symbol denotes a c-function used in grid generation. A tilde (~) over a symbol denotes a λ-function used in grid generation. Primes denote a derivative with respect to the argument.

Analysis

Surface Equations

The analysis is described as it applies to the basic lofting problem in its simplest form: a surface component is to be designed so that it varies gradually and smoothly from a given initial cross-sectional shape to a different specified terminal or base shape. Such a component might represent, for example, a forebody, a wing, or a duct. The direction of variation is taken to be the x-direction, with the two end shapes specified in y-z planes (fig. 1(a)).

Neglecting for the moment the variation in cross-sectional size, consider first only the shape variation.

Suppose the initial shape can be represented in parametric form with parameter t:

$$\left.\begin{aligned} y_1 &= y_1(t) \\ z_1 &= z_1(t) \end{aligned}\right\} \qquad (t_a < t < t_b) \tag{1}$$

and the terminal cross section is also representable in parametric form with the same t domain (t_a, t_b):

$$y_2 = y_2(t) \tag{2a}$$

$$z_2 = z_2(t) \tag{2b}$$

(See fig. 1(b).)

For example, if the cross sections are appropriately represented in polar form, then

$$\left.\begin{aligned} y_1 &= R_1(\theta)\cos\theta \\ z_1 &= R_1(\theta)\sin\theta \end{aligned}\right\} \qquad (0 < \theta < 2\pi)$$

with similar expressions for y_2 and z_2. The x-variable is now normalized by

$$x_n = \frac{x - x_1}{x_2 - x_1} \tag{3}$$

and a parameter $c_n(x_n)$ is defined such that c_n varies from 0 to 1 as x_n varies continuously and monotonically from 0 to 1 (i.e., a homotopy parameter). Then define c by

$$c(x) \equiv c_n[x_n(x)] \tag{4}$$

Thus, $c(x_1) = 0$ and $c(x_2) = 1$. The function $c(x_n)$ is usually specified to be smooth and monotonic. A typical expression for c_n might be

$$c_n(x_n) = x_n^m \tag{5}$$

with m as an adjustable design parameter. A transition surface representing a smooth blending of the two end shapes is defined by the functions

$$y(x,t) = [1 - c(x)]y_1(t) + c(x)\ y_2(t) \tag{6a}$$

$$z(x,t) = [1 - c(x)]z_1(t) + c(x)\ z_2(t) \tag{6b}$$

Finally, the size variation of the surface is prescribed by introducing an independent scaling function $\lambda(x)$ which is specified to be smooth and nonnegative but not necessarily monotonic. Thus, the lofted surface is defined by the equations

$$y(x,t) = \lambda(x)\{[1 - c(x)]y_1(t) + c(x)\ y_2(t)\} \tag{7a}$$

$$z(x,t) = \lambda(x)\{[1 - c(x)]z_1(t) + c(x)\ z_2(t)\} \tag{7b}$$

A somewhat different type of transition surface is defined by

$$y(x,t) = \lambda y_1^{(1-c)} y_2^c \tag{8a}$$

$$z(x,t) = \lambda z_1^{(1-c)} y_2^c \tag{8b}$$

where c and λ are functions of x, and y_1, y_2, z_1, and z_2 are all functions of t. Other, more complicated forms of transition surface equations may also be defined. The vector form of the surface equation is

$$\mathbf{r}(x,t) = x\hat{i} + y(x,t)\hat{j} + z(x,t)\hat{k} \tag{9}$$

Computation of Surface Parameters

Equation (9) together with equation (7) or (8), defines the transition surface in terms of four functions, each defined as a function of a single independent variable. The two end shapes (y_1, z_1) and (y_2, z_2) depend only on t, whereas the shape variation function c and the size variation function λ depend only on x. Therefore, the derivatives of the surface vector $\mathbf{r}(x,t)$ can be computed in terms of the derivatives of these individual functions. Thus,

$$\begin{aligned} \mathbf{r}_x(x,t) = \hat{i} &+ [(\lambda_x/\lambda)\ y(x,t) + \lambda c_x(y_2 - y_1)]\hat{j} \\ &+ [(\lambda_x/\lambda)\ z(x,t) + \lambda c_x(z_2 - z_1)]\hat{k} \end{aligned} \tag{10}$$

and

$$\begin{aligned} \mathbf{r}_t(x,t) = 0\hat{i} &+ \lambda[(1-c)y_{1_t} + cy_{2_t}]\hat{j} \\ &+ \lambda[(1-c)z_{1_t} + cz_{2_t}]\hat{k} \end{aligned} \tag{11}$$

(See fig. 1(c).) In equations (10) and (11), c and λ are functions of x, while y_1, y_2, z_1, and z_2 are functions of t. With these equations, one can directly compute the surface parameters that depend only on the first derivatives, such as the metric coefficients

$$E = \mathbf{r}_x \cdot \mathbf{r}_x \tag{12a}$$

$$F = \mathbf{r}_x \cdot \mathbf{r}_t \tag{12b}$$

$$G = \mathbf{r}_t \cdot \mathbf{r}_t \tag{12c}$$

the surface normal

$$\hat{N} = \frac{\mathbf{r}_x \times \mathbf{r}_t}{\sqrt{EG - F^2}} \tag{13}$$

and the local area element

$$dA = \sqrt{EG - F^2}\ dx\ dt \tag{14}$$

By differentiating equations (10) and (11) again, the second derivatives $\mathbf{r}_{xx}$, $\mathbf{r}_{xt}$, and $\mathbf{r}_{tt}$ can be obtained. From these, the local curvature coefficients can be calculated as well as surface parameters such as the principal curvature, mean and total curvature, and curvature directions according to the basic differential geometry formulas. (See, for example, ref. 3.)

Computed Example

An example of a transition surface is shown in figure 2. This surface, which might represent the upper surface of a blended wing-body combination, was generated by equations (7) and (9) with the following choice of variables. For the initial cross section at $x_1 = 0$,

$$\left.\begin{aligned} y_1(t) &= t \\ z_1(t) &= \frac{\sqrt{1-t^2}}{3} \end{aligned}\right\} \quad (-1 \le t \le 1)$$

For the final cross section, at $x_2 = 5.0$,

$$\begin{aligned} y_2(t) &= t && (-1 \le t \le 1) \\ z_2(t) &= \sqrt{(0.317)^2 - t^2} && (|t| \le 0.317) \\ z_2(t) &= -0.2(|t| - 0.317) && (1 \ge |t| \ge 0.317) \end{aligned}$$

The x-coordinate was nondimensionalized as follows:

$$x_n \equiv \frac{x}{x_2}$$

A linear variation of the shape transition was prescribed as follows:

$$c_n(x_n) = x_n$$

but, for this particular example, a more general version of the size variation function

$$\begin{aligned} \lambda(x_n) = \lambda_2(&1.6x_n - 5.316x_n^2 \\ &+ 9.133x_n^3 - 4.417x_n^4) \end{aligned}$$

was required to provide the smooth transition surface shown in figure 2(b).

Use of Digitized Input

In the event that one of the specified cross-sectional end shapes is difficult to describe analytically, it is necessary to represent it numerically (for example, by means of digitized data). In this case, the data must be smoothed in order to avoid the irregularity and oscillation of the derivatives that are characteristic of unsmoothed data. This smoothing is accomplished through the use of b-splines. (Details on b-spline theory and techniques are given in ref. 4.) The numerical cross-sectional data are displayed graphically along with the first two numerical derivatives (fig. 3(a)). The various b-spline parameters are adjusted interactively until a shape is obtained that represents a satisfactory smooth approximation to the original input shape and its derivatives are free of spurious oscillation (fig. 3(b)). These numerical functions describing the cross-sectional shape can then be used in the transition surface equations (eqs. (7) to (11)), with the other end shape specified either analytically or numerically.

Similarly, the shape- and size-variation functions, $c(x)$ and $\lambda(x)$, could be specified numerically. However, since these variations are normally smooth and gradual for aerodynamic shapes, analytic expressions are normally satisfactory for their representation.

It should be emphasized that, if one or more of the basic geometry functions is defined numerically but smoothed so that the required derivatives are meaningful, then the surface parameters can still be computed from the transition surface formulas (eqs. (7) to (9)). This formulation, which represents an analytic combination of numerical and analytic functions, is termed "semianalytic."

Specifying an Intermediate Cross-Sectional Shape

A designer may need to define a surface which is to vary gradually in cross-sectional shape but in such a way that intermediate cross sections cannot reasonably be described as a blending of the two end shapes. Two approaches to this problem are discussed. The first approach is to define a single transition surface that includes the specified intermediate cross-sectional shape. Denote this cross section at intermediate axial station x_3 by $y_3(t)$, $z_3(t)$ with t having the same domain as for the two end shapes. For the sake of simplicity in notation, x is normalized so that

$$x_1 = 0$$

$$x_2 = 1$$

$$0 < x_3 < 1$$

Define

$$x_m \equiv 1 - x_3$$

Then the simplest surface that satisfies the prescribed conditions is given by

$$\begin{aligned} y(x,t) = \lambda(x)\Bigg\{\Bigg[1 - \frac{1+x_3}{x_3}x &+ \frac{x^2}{x_3}\Bigg] y_1(t) - \frac{x_3 - x}{x_m} x\, y_2(t) \\ &+ \frac{1-x}{x_3 x_m} x\, y_3(t)\Bigg\} \end{aligned} \tag{15}$$

with a similar expression for $z(x,t)$.

This formula satisfies the required conditions, but it contains no free parameters (other than $\lambda(x)$) to permit further flexibility in design. Some freedom in design could be introduced by the addition of higher degree terms in x, but at the expense of greater

complexity and with the risk of creating a waviness in the surface.

The second approach for introducing a specified cross-sectional shape between the two given end shapes is to treat the surface as two transition surfaces joined end to end at x_3. Define the new normalized axial variables as

$$x_a \equiv \frac{x - x_1}{x_3 - x_1} \tag{16a}$$

$$x_b \equiv \frac{x - x_3}{x_2 - x_3} \tag{16b}$$

Since multiplication by a smooth scale function $\lambda(x)$ will not affect the differentiability of the resulting surface, the two unscaled transition surfaces will be considered:

$$y_a(x_a, t) = (1 - c_a)y_1 + c_a y_3 \tag{17a}$$

$$z_a(x_a, t) = (1 - c_a)z_1 + c_a z_3 \tag{17b}$$

$$y_b(x_b, t) = (1 - c_b)y_3 + c_b y_2 \tag{18a}$$

$$z_b(x_b, t) = (1 - c_b)z_3 + c_b z_2 \tag{18b}$$

At the juncture location x_3,

$$c_a = 1, \; c_b = 0$$

$$x_a = 1, \; x_b = 0$$

$$y_a = y_b \tag{19}$$

$$y_{a_t} = y_{b_t} \tag{20}$$

$$y_{a_x} = (y_3 - y_1)\frac{dc_a}{dx_a}\frac{dx_a}{dx} = \frac{y_3 - y_1}{x_3 - x_1}c'_a \tag{21a}$$

$$y_{b_x} = \frac{y_2 - y_3}{x_2 - x_3}c'_b \tag{21b}$$

with similar expressons for the z-coordinate. In equations (17), (18), and (19), c_a and c_b are functions of x, whereas y_1, y_2, y_3, x_1, x_2, and x_3 are functions of t.

From equations (21), it is apparent that the first derivative with respect to x is continuous at x_3 only if $c_a(x_a)$ and $c_b(x_b)$ are defined so that

$$c'_a(1) = c'_b(0) = 0 \tag{22}$$

except in the unusual circumstance that the two functions $y_2(t)$ and $y_1(t)$ are identically equal, in which case the requirement is that, at x_3,

$$c'_a(1) = -\frac{x_3 - x_1}{x_2 - x_3}c'_b(0) \tag{23}$$

For this equation to be satisfied, one of the shape transition functions would fail to meet the monotonicity condition.

If the second derivative were required to be continuous at x_3, then in addition to equation (22), the condition

$$c''_a(1) = c''_b(0) = 0 \tag{24}$$

would be enforced.

If a fourth cross section is specified at x_4 (where $x_3 < x_4 < x_2$) so that a third transition surface (with transition function c_c) between x_3 and x_4 is required, then it must satisfy the conditions

$$c'_c(0) = c'_c(1) = 0 \tag{25}$$

in order to ensure continuity of the first derivative at both ends of the interval.

In theory, this procedure could be continued indefinitely with the insertion of an arbitrary number of specified intermediate cross sections. However, the requirement that the shapes be "lined-up" at the juncture according to equation (25) would tend to lead rapidly to the undesirable waviness of the surface.

Combining Surfaces

After each individual component has been represented in analytic or semianalytic form, there remains the problem of synthesizing these components into a configuration. Discussion of all the various approaches to this problem is beyond the scope of the present paper, but one technique that has been used effectively is simple superposition. Its application in the present context is illustrated with a particular example—that of superimposing a canopy onto a fuselage (fig. 4(a)). Let the equation for the upper surface of the fuselage be

$$\mathbf{r}_f(x, t_f) = x\hat{i} + y_f(x, t_f)\hat{j} + z_f(x, t_f)\hat{k} \qquad (0 < x < x_2) \tag{26a}$$

and let the equation for the canopy surface be

$$\mathbf{r}_s(x, t_s) = x\hat{i} + y_s(x, t_s)\hat{j} + z_s(x, t_s)\hat{k} \qquad (0 < x_1 < x < x_3 < x_2) \tag{26b}$$

For purposes of illustration, assume that the range of t is $(-1, +1)$ for both $\mathbf{r}_f$ and $\mathbf{r}_s$. Then $t = -1$ and $t = +1$ represent the lateral extremes of the components, which are symmetric about $t = 0$. Let x_1 denote the axial station at which the canopy surface is to be initiated. Then, for any $x > x_1$, $y_s(x - x_1, 1)$ is calculated. Then, for this value of y, the corresponding value of t for the fuselage surface is calculated (fig. 4(a)). Suppose, for example, that

$$y_f(x, t_f) = \lambda_f(x)t_f \tag{27a}$$

$$y_s(x-x_1, t_s) = \lambda_s(x-x_1)t_s \qquad (27b)$$

$$y_s(x-x_1, 1) = \lambda_s(x-x_1) \qquad (28)$$

Then, for the fuselage surface, the corresponding value of t_f is found by substituting relation (28) into relation (27a)

$$t_\ell = \frac{\lambda_s(x-x_1)}{\lambda_f(x)} \qquad (29)$$

Such a boundary value, t_ℓ, can be determined for each value of $x > x_1$. If an analytic expression such as equation (29) cannot be obtained, t_ℓ must be computed numerically. Then the synthesized surface is defined by the relations

$$\mathbf{r}(x, t_f) = \mathbf{r}_f(x, t_f) \qquad (x < x_1) \qquad (30a)$$

$$\mathbf{r}(x, t_f) = \mathbf{r}_f(x, t_f) \qquad (x \geq x_1;\ |t_f| > |t_\ell(x)|) \qquad (30b)$$

$$\mathbf{r}(x, t_s) = x\hat{i} + y_s(x-x_1, t_s)\hat{j} + [z_f(x, t_\ell) + z_s(x-x_1, t_s)]\hat{k} \qquad (x \geq x_1;\ |t_f| \leq |t_\ell(x)|) \qquad (30c)$$

Figure 4(b) shows a surface formed by a synthesis of several components in this manner to form a fuselage-like geometry.

Discussion Regarding Applications

Aerodynamic Design

The transition surface equations (eqs. (7) to (9)) were originally developed as a means for rapid calculation of surfaces generated by a lofting procedure. The two end cross sections are specified by the designer, and the intermediate cross sections are computed from equation (9) as x = Constant lines. These can be displayed graphically; and the shape and scale functions, $c(x)$ and $\lambda(x)$, can be varied interactively to obtain the desired transition. The lofting lines are the t = Constant lines. Since the two end shapes are specified so that there is a natural one-to-one t-correspondence, this correspondence holds throughout the transition, and consequently there is no problem with lofting lines developing waves or crossing each other.

Grid generation

A single transition surface such as that shown in figure 2(b) is especially easy to grid for purposes of flow calculations. The (x, t) coordinate lines form a natural surface grid. The external field can be gridded by a simple extension of the homotopic procedure that is used to generate the surface itself.

For calculation of supersonic flow over such a surface, a quasi-two-dimensional grid is sufficient. An outer boundary surface must be specified. If the configuration is contained within a duct (e.g., a wind-tunnel test section), the duct wall serves this purpose, but otherwise a simple shape, such as a cylinder, is arbitrarily chosen. This outer boundary shape is also represented as a transition surface with the same distribution of the t and x variables as used to describe the inner surface. Then the grid is generated by defining, at each constant x-station, a homotopic variation from the inner surface y_i, z_i to the outer boundary y_o, z_o. Denote this homotopy parameter by η, and the shape transition function by c^*. Thus,

$$c^*(\eta) = 0 \qquad (\eta = 0) \qquad (31a)$$

$$c^*(\eta) = 1 \qquad (\eta = 1) \qquad (31b)$$

This function is taken to be independent of x; it is the same at each x-station.

Now denote the size variation function by λ^* so that $\lambda_i < \lambda^* < \lambda_o$. Since the size of the inner surface, and possibly the outer boundary also, varies with x, λ^* cannot be independent of x. It can, however, be expressed in terms of a normalized function $\tilde{\lambda}$ by

$$\lambda^* = \lambda_i + \tilde{\lambda}(\lambda_o - \lambda_i) \qquad (32)$$

so that

$$\tilde{\lambda}(\eta) = 0 \qquad (\eta = 0)$$

$$\tilde{\lambda}(\eta) = 1 \qquad (\eta = 1)$$

and $\tilde{\lambda}$ is independent of x. By defining the grid at each x-station in terms of these functions, $c^*(\eta)$ and $\tilde{\lambda}(\eta)$, a natural correspondence is established between grid points at the various x-stations. If both inner and outer boundaries vary smoothly with x, the corresponding grid-point locations will vary smoothly. Figure 5 shows a grid generated in this manner for a cross section of a transition surface similar to that of figure 2(b).

For some flow calculations, such a quasi-two-dimensional grid is not always adequate. If the grid structure is required to reflect the influence of the body shape upstream of the nose, a fully three-dimensional grid can be defined as follows. Take the average x-station $\frac{x_1+x_2}{2}$ for the surface as the origin so that the surface is now defined on the domain

$$-\xi_{i,l} \leq \xi < \xi_{i,l} \qquad (-1 \leq t \leq 1)$$

For the outer boundary shape, define an appropriate convex surface (e.g., ellipsoid) on the same ξ, t domain with the same distribution of the ξ and t variables as for the inner surface. The outer boundary shape is obtained by multiplying this surface $\mathbf{r}(\xi, t)$ by a large scale factor λ_o. The grid homotopy parameter is again denoted by η; the shape transition

function, by $c^*(\eta)$; and the size transition, by $\lambda^*(\eta)$ (where $1 < \lambda^* < \lambda_o$). Also a homotopic function $\mu(\xi)$ is defined such that μ varies monotonically from 0 to 1 as $|\xi|$ varies from 0 to 1. Then the grid-point locations are given by

$$x(\xi,\eta) = \lambda^*(\eta)\ \mu(\xi) \tag{33a}$$

$$y(\xi,t,\eta) = \lambda^*(\eta)\{[1 - c^*(\eta)]y_i(\xi,t) + c^*(\eta)\ y_o(\eta,t)\} \tag{33b}$$

$$z(\xi,t,\eta) = \lambda^*(\eta)\{[1 - c^*(\eta)]z_i(\xi,t) + c^*(\eta)\ z_o(\xi,t)\} \tag{33c}$$

As in the quasi-two-dimensional case, considerable flexibility is permitted in designing the grid by independent control of the shape and size variation functions.

A grid-type structure generated by equations (33) is illustrated in figure 6. Figure 6(a) shows a tapered, cambered wing. Figure 6(b) shows two of the ξ = Constant sections viewed from the wing root. Figure 6(c) shows a t = Constant section viewed from the front of the wing. A blow-up of the circumscribed region in figure 6(c) is shown in figure 6(d) to display the shape of the ξ = Constant lines near the surface.

Concluding Remarks

Equations for the semianalytic representation of a class of surfaces that vary gradually in cross-sectional shape have been presented. It was demonstrated that basic surface geometry parameters can easily be calculated with such a representation. Some methods for fitting together and superimposing the surfaces were described. Also included was a brief discussion of the application of the theory in various contexts such as computerized lofting of aerodynamic surfaces and grid generation.

NASA Langley Research Center
Hampton, VA 23665
December 18, 1984

References

1. Coons, Steven A.: *Surfaces for Computer-Aided Design of Space Forms*, MAC-TR-41 (Contract No. AF-33(600)-42859), Massachusetts Inst. Technol., June 1967. (Available from DTIC as AD 663 504.)
2. Barger, Raymond L.: *A Procedure for Designing Forebodies With Contraints on Cross-Section Shape and Axial Area Distribution.* NASA TP-1881, 1981.
3. Struik, Dirk J.: *Differential Geometry.* Addison-Wesley Pub. Co., Inc., c.1950.
4. Rogers, David F.; and Adams, J. Alan: *Mathematical Elements for Computer Graphics.* McGraw-Hill, Inc., c.1976.

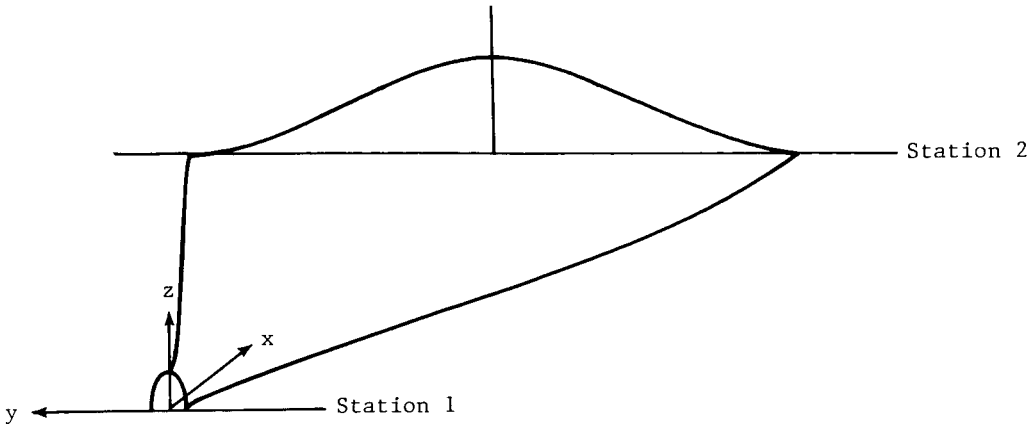

(a) Perspective view of lofted surface.

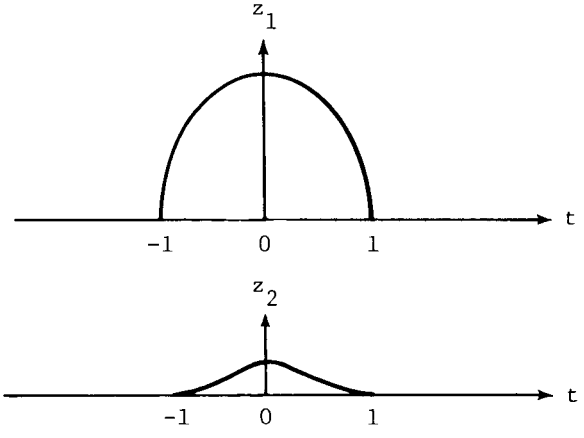

(b) Normalized end sections.

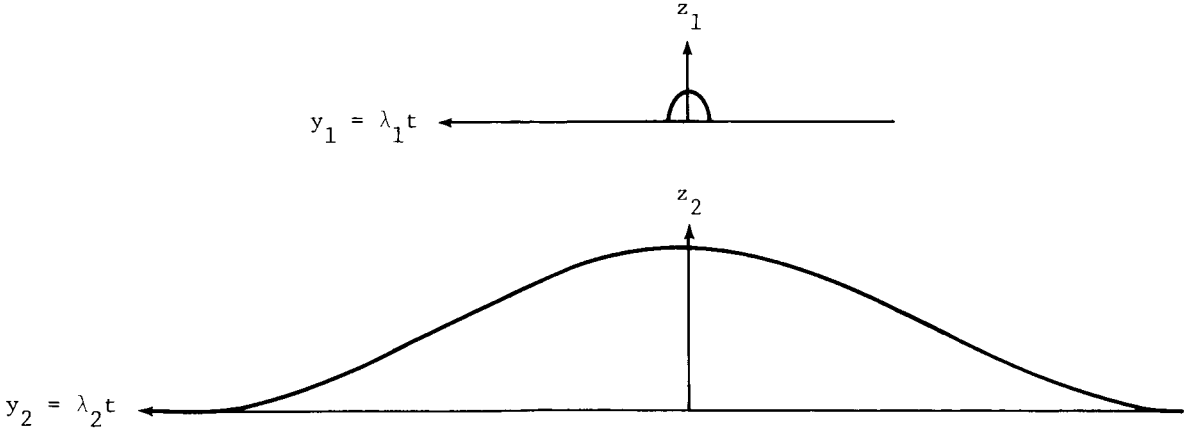

(c) Scaled end sections.

Figure 1. Analytic lofting: end sections and lofted surface.

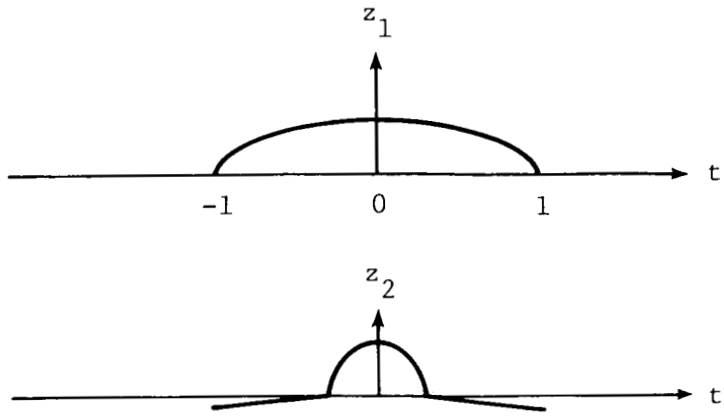

(a) Unscaled end sections.

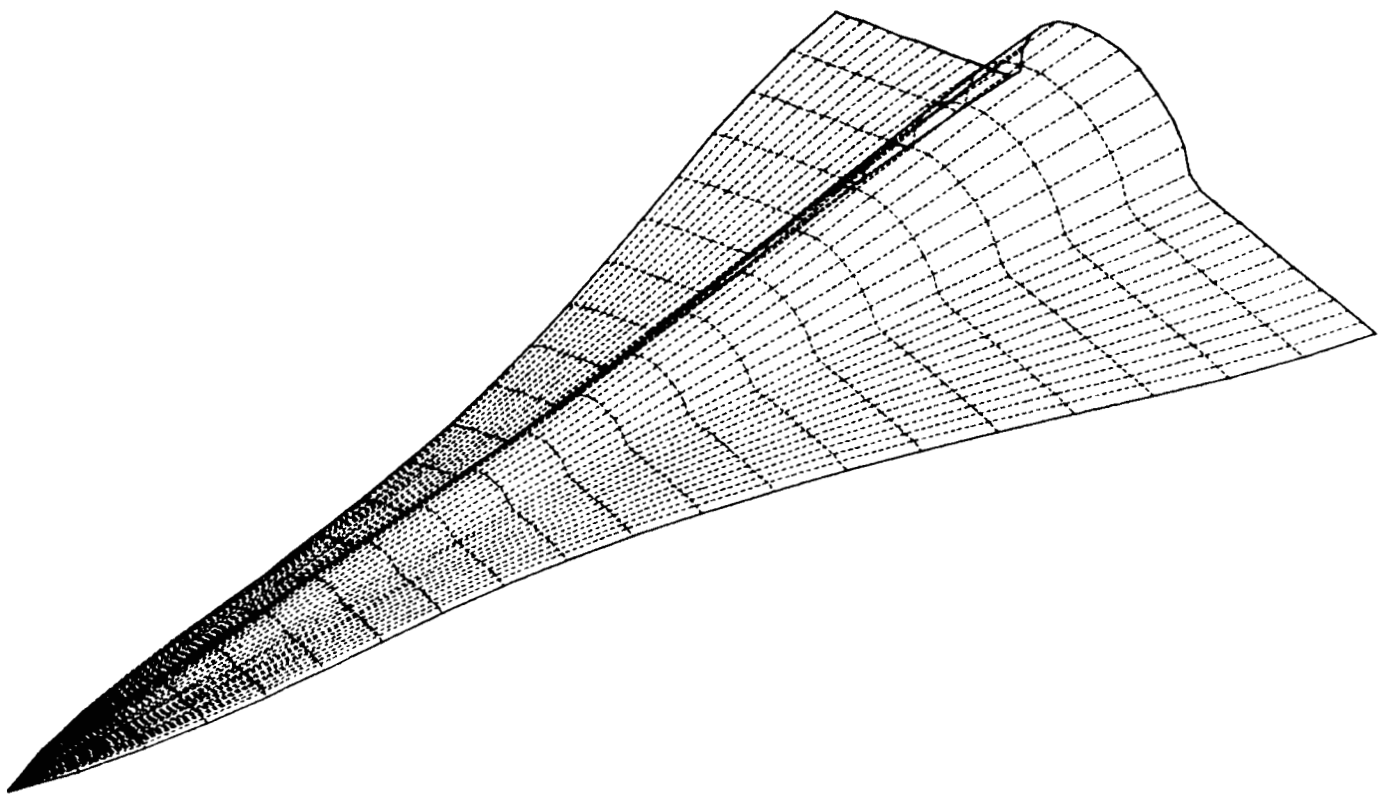

(b) Perspective view of surface.

Figure 2. Blended wing-body combination generated as a transition surface.

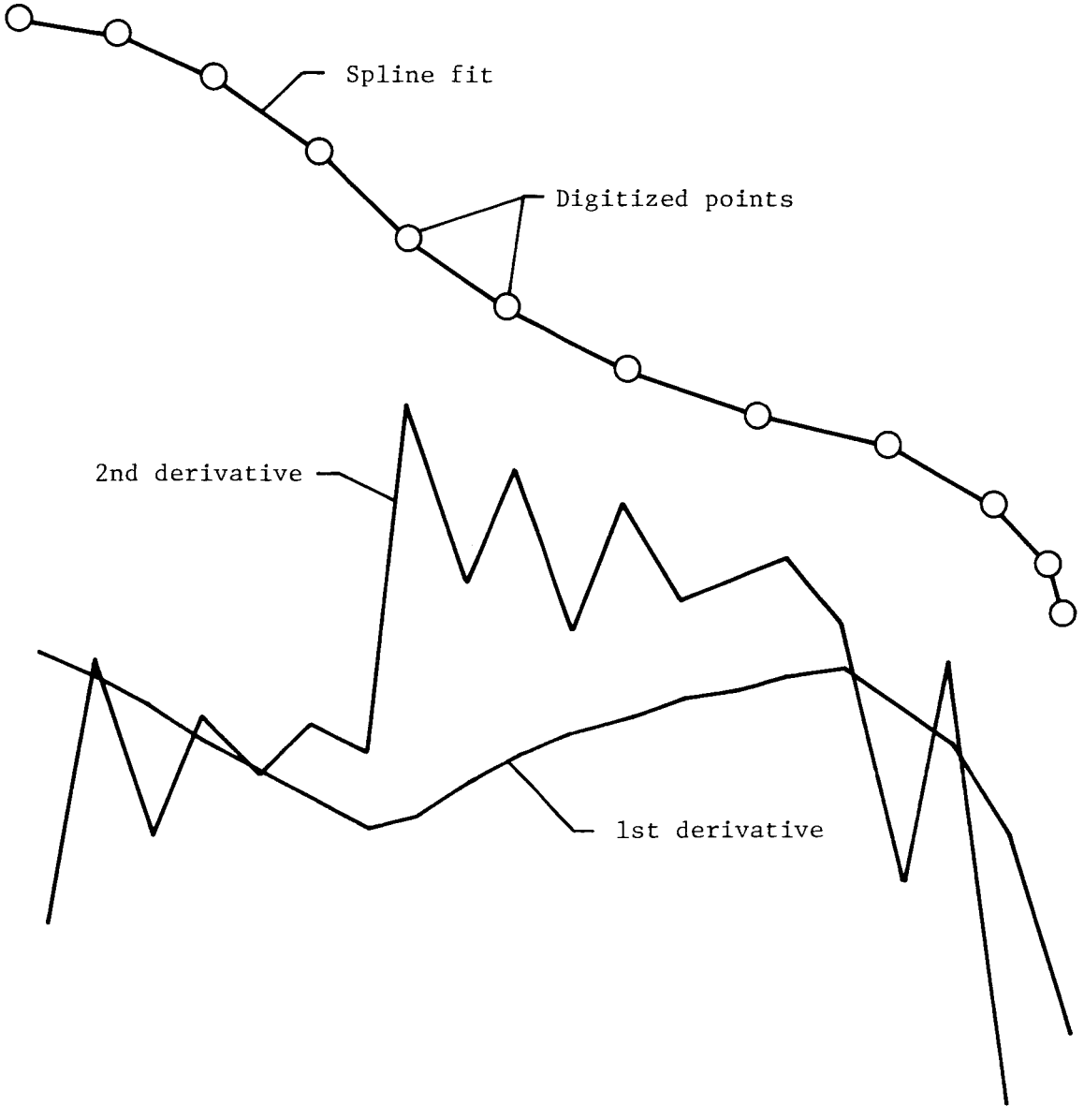

(a) Linear 20-point fit.

Figure 3. Curve fit and numerical derivatives for digitized cross section.

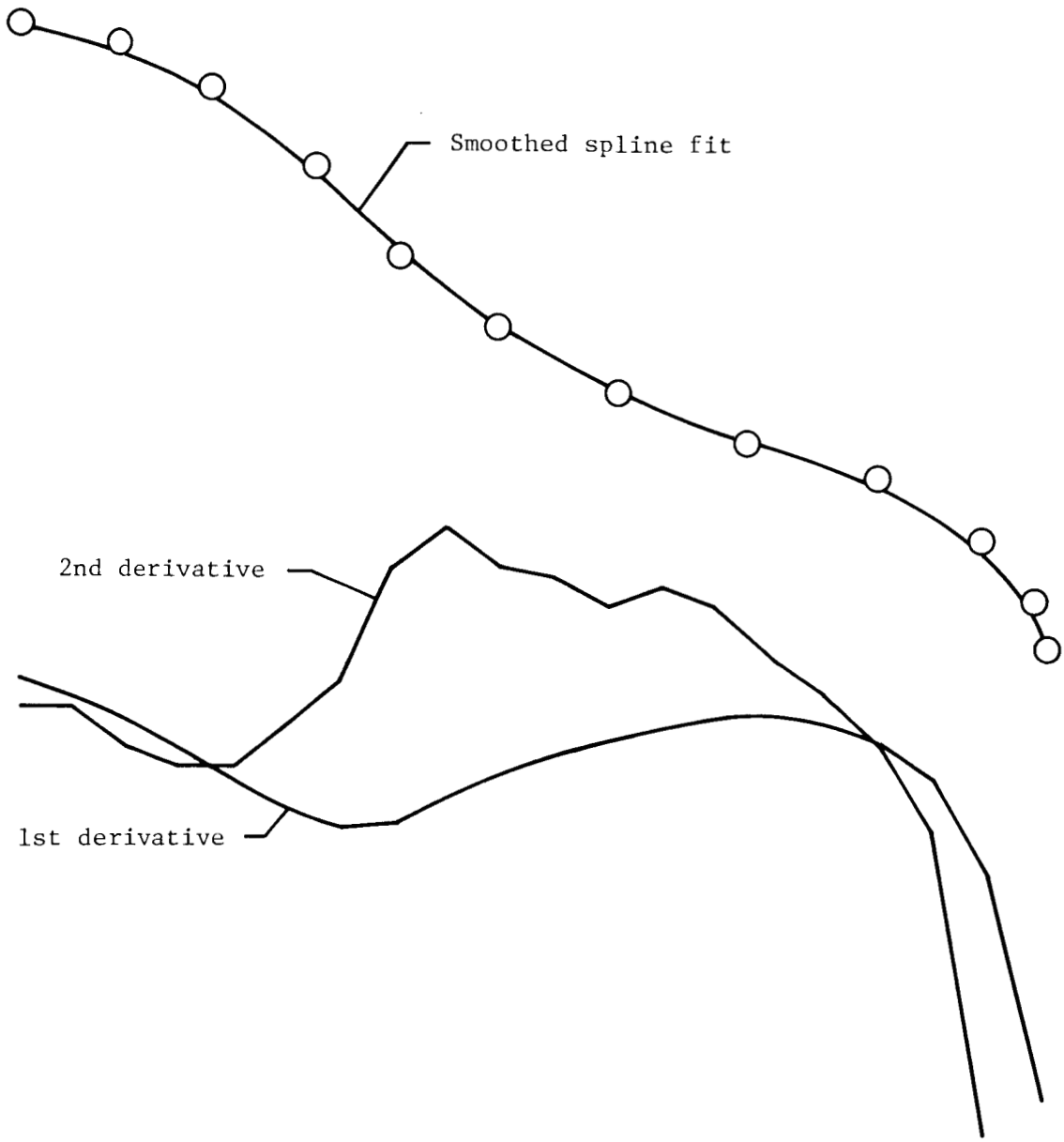

(b) 20-point fifth-order local *b*-spline fit.

Figure 3. Concluded.

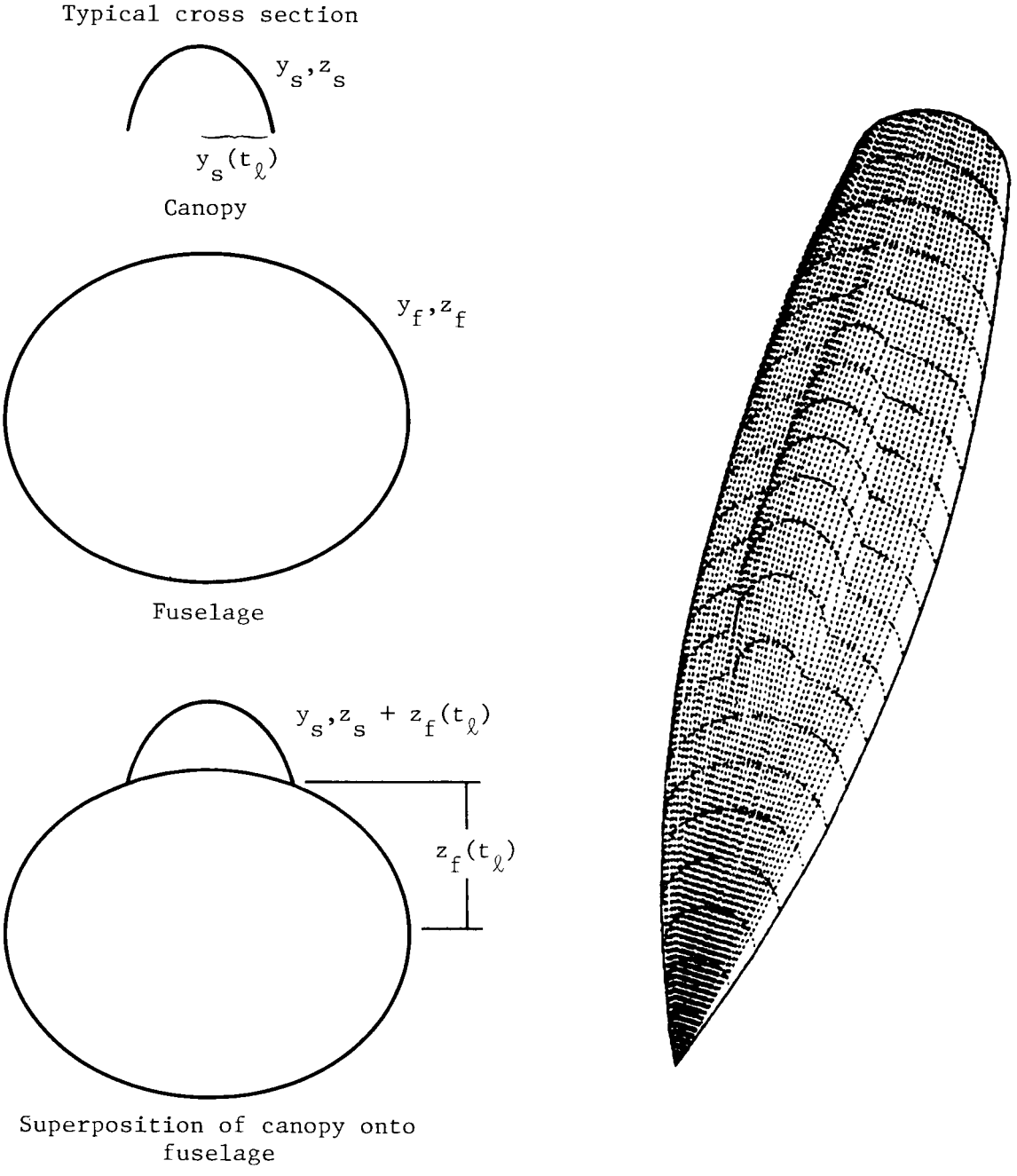

(a) Canopy superimposed on fuselage.

Figure 4. Superposition of transition surfaces.

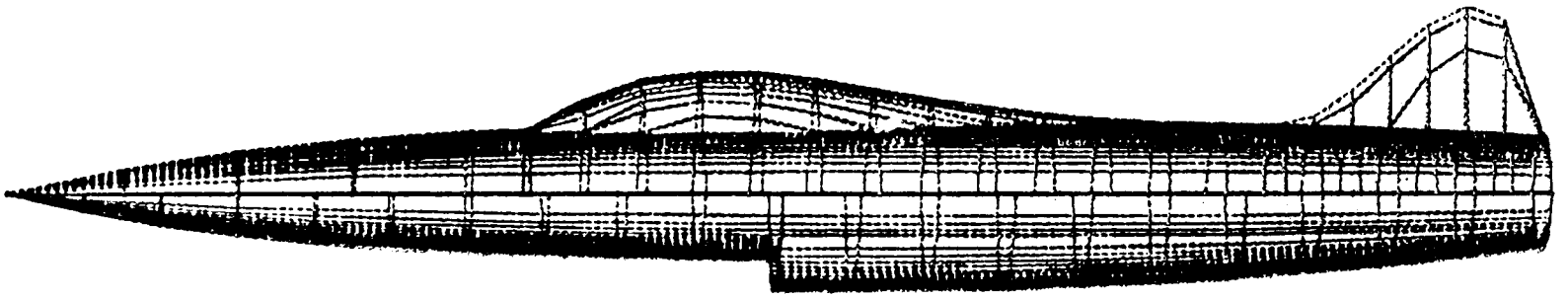

(b) Combination of several surfaces.

Figure 4. Concluded.

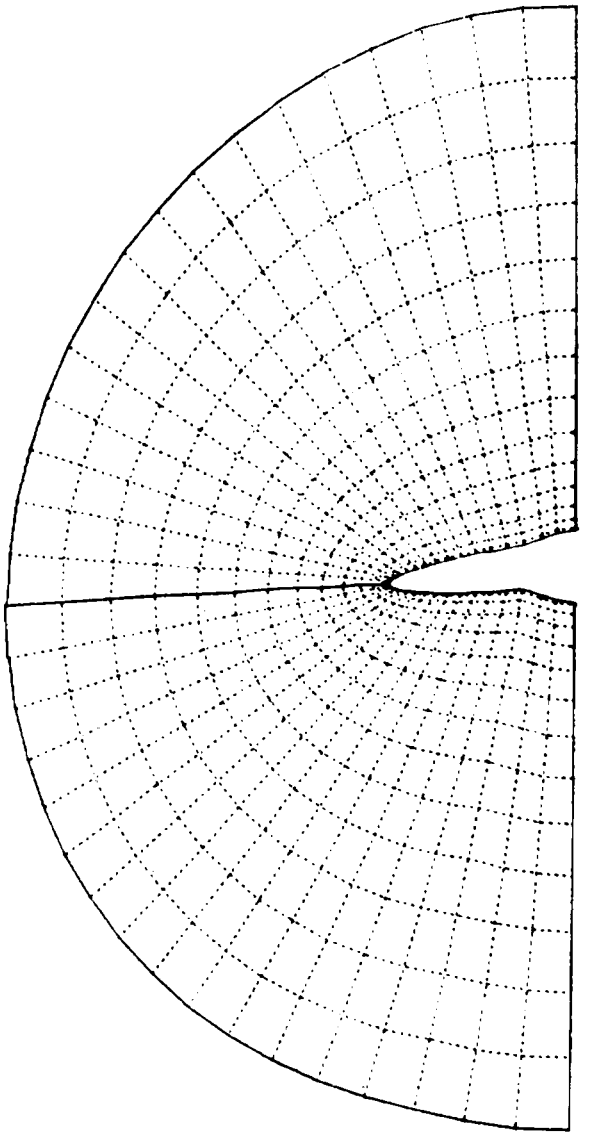

Figure 5. Computational grid at single axial station.

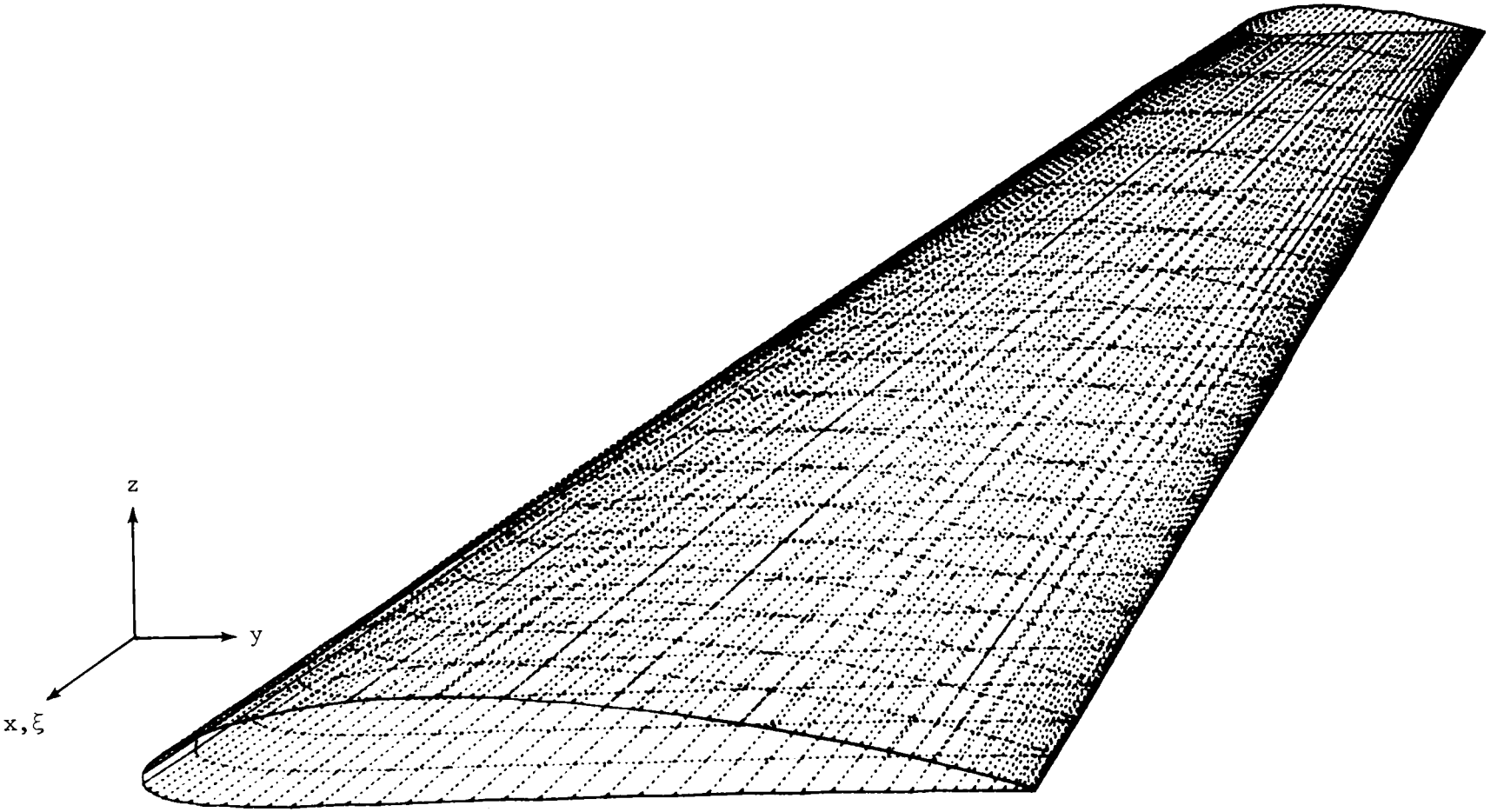

(a) Basic surface: tapered, cambered wing.

Figure 6. Sample three-dimensional grid-type structure for transition surface.

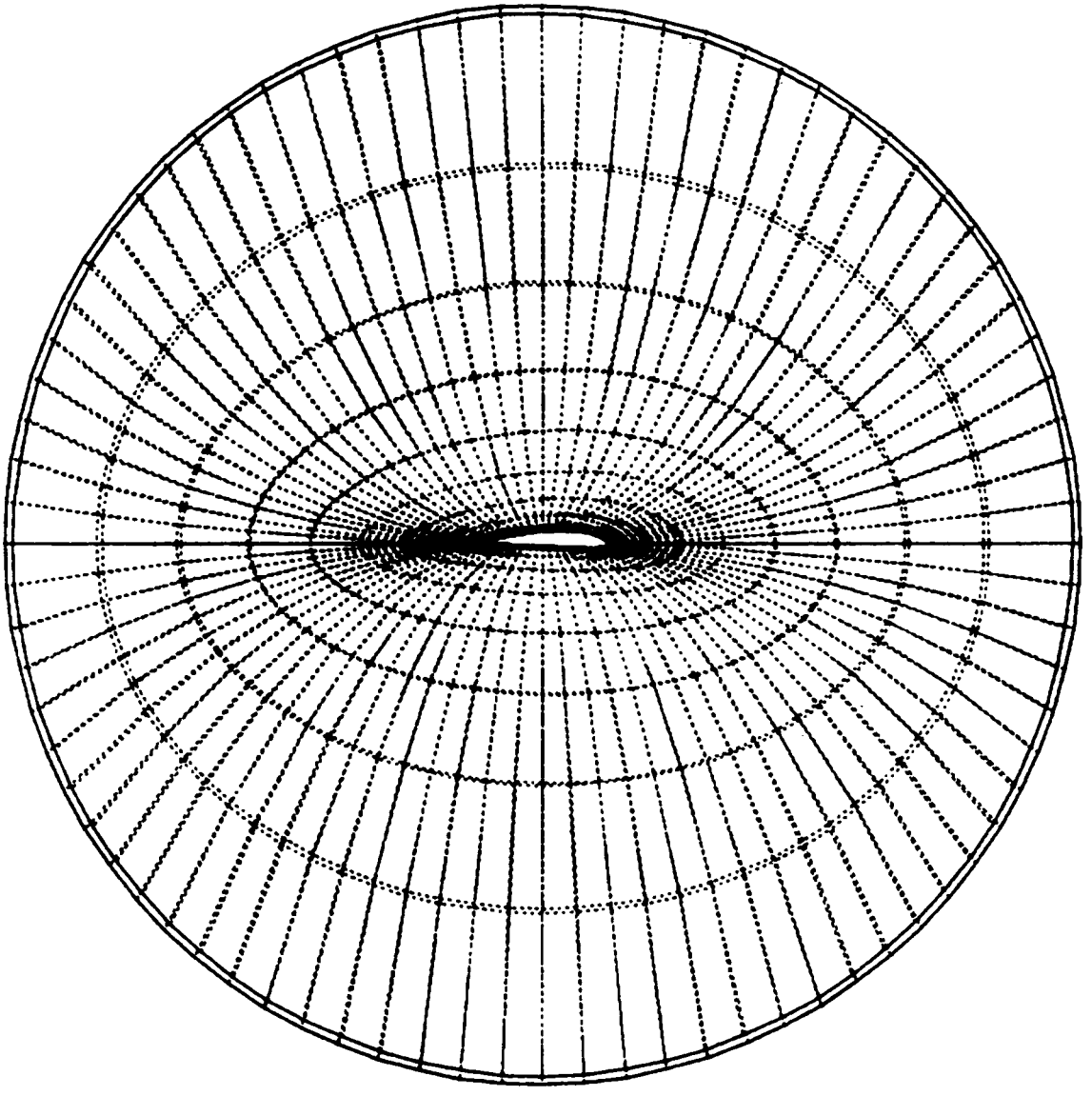

(b) End view (from wing root) of two ξ = Constant sections.

Figure 6. Continued.

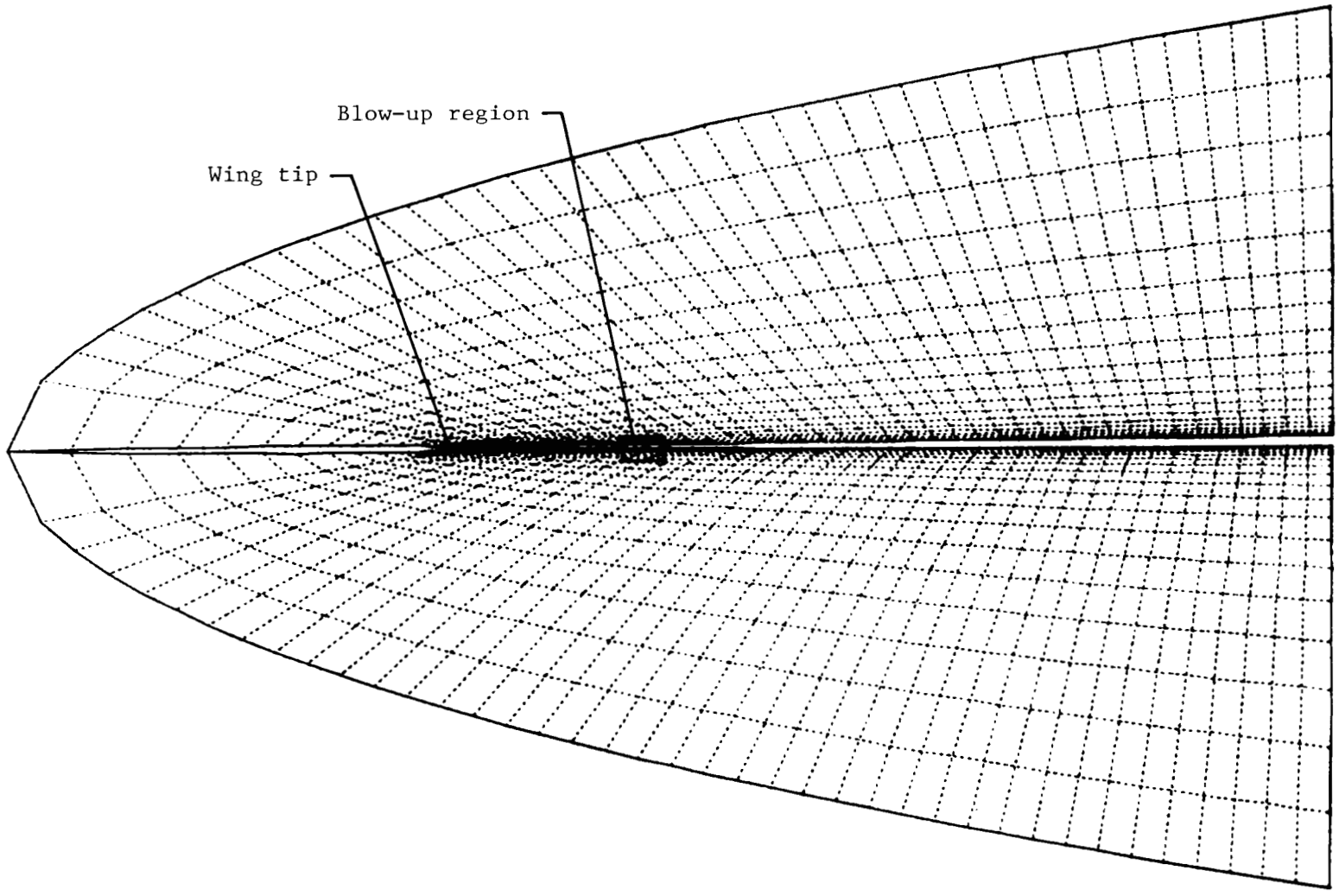

(c) t = Constant section viewed from front of wing.

Figure 6. Continued.

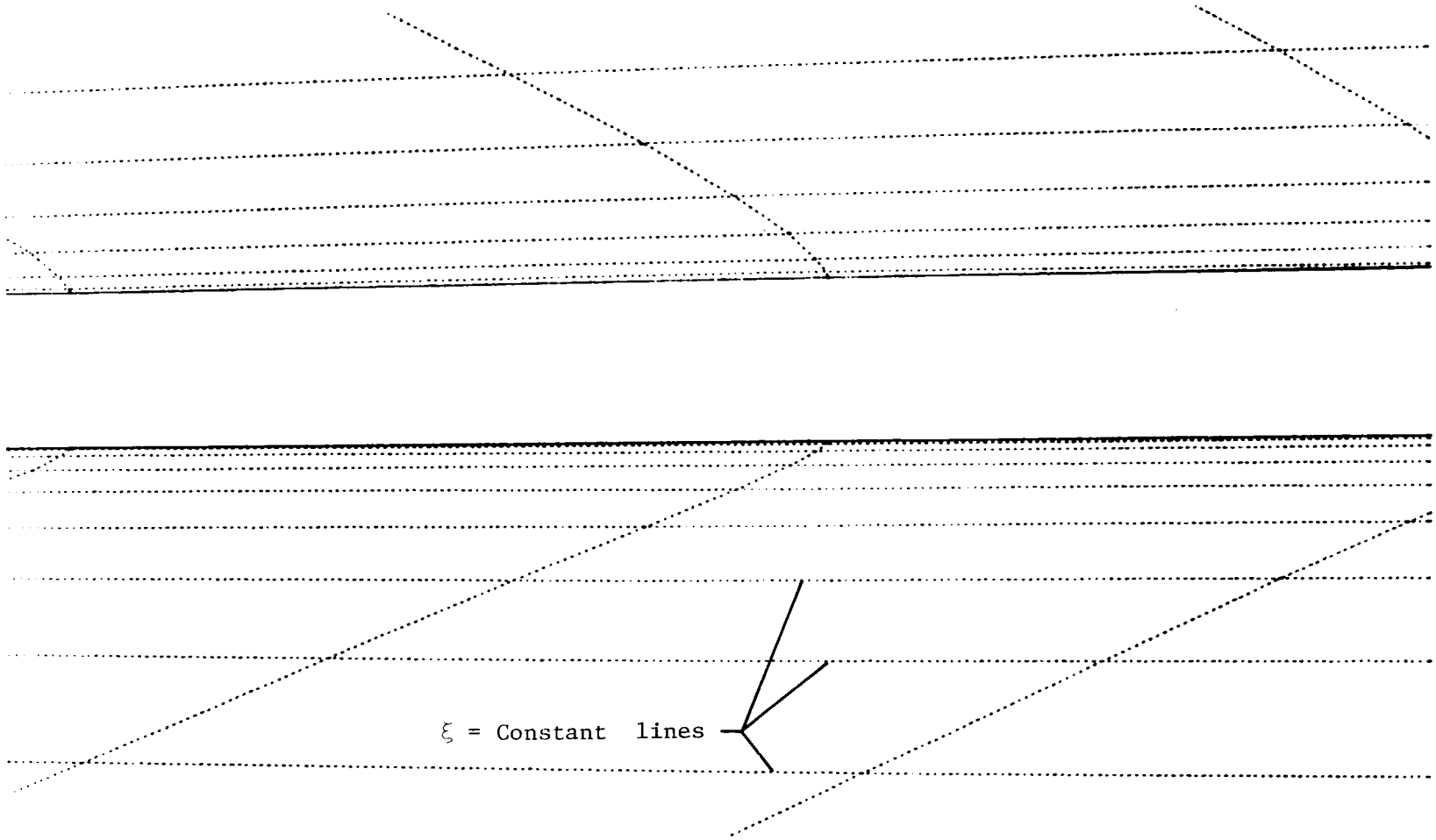

(d) Blow-up of block indicated in figure 6(c).

Figure 6. Concluded.

1. Report No.	2. Government Accession No.	3. Recipient's Catalog No.
NASA TP-2413		

4. Title and Subtitle	5. Report Date
Semianalytic Modeling of Aerodynamic Shapes	April 1985
	6. Performing Organization Code: 505-43-23-08
7. Author(s): Raymond L. Barger and Mary S. Adams	8. Performing Organization Report No.: L-15879
9. Performing Organization Name and Address: NASA Langley Research Center, Hampton, VA 23665	10. Work Unit No.
	11. Contract or Grant No.
12. Sponsoring Agency Name and Address: National Aeronautics and Space Administration, Washington, DC 20546	13. Type of Report and Period Covered: Technical Paper
	14. Sponsoring Agency Code

15. Supplementary Notes

16. Abstract

Equations for the semianalytic representation of a class of surfaces that vary smoothly in cross-sectional shape are presented. Some methods for fitting together and superimposing such surfaces are described. A brief discussion is also included of the application of the theory in various contexts such as computerized lofting of aerodynamic surfaces and grid generation.

17. Key Words (Suggested by Authors(s))
Aerodynamic modeling
Analytic shapes
Computer lofting
Surface modeling
Surface parameters
Surface geometry

18. Distribution Statement
Unclassified—Unlimited

Subject Category 02

19. Security Classif.(of this report)	20. Security Classif.(of this page)	21. No. of Pages	22. Price
Unclassified	Unclassified	18	A02

For sale by the National Technical Information Service, Springfield, Virginia 22161

NASA-Langley, 1985

2 2 1U,A, 850329 S00161DS
DEPT OF THE AIR FORCE
ARNOLD ENG DEVELOPMENT CENTER(AFSC)
ATTN: LIBRARY/DOCUMENTS
ARNOLD AF STA TN 37389